Virologica Sinica 38 (2023) 47–55

Contents lists available at ScienceDirect

Virologica Sinica

journal homepage: www.keaipublishing.com/en/journals/virologica-sinica
www.virosin.org

Research Article

Enhanced pathogenicity and transmissibility of H9N2 avian influenza virus in mammals by hemagglutinin mutations combined with PB2-627K

Kaituo Liu [a,b,c,d], Yaqian Guo [b], Huafen Zheng [b], Zhuxing Ji [b], Miao Cai [b], Ruyi Gao [b,c,d], Pinghu Zhang [e], Xiaowen Liu [b,c,d], Xiulong Xu [a,b,c,d], Xiaoquan Wang [a,b,c,d,*], Xiufan Liu [a,b,c,d,*]

[a] Joint International Research Laboratory of Agriculture and Agri-Product Safety, The Ministry of Education of China, Yangzhou University, Yangzhou, 225009, China
[b] Animal Infectious Disease Laboratory, College of Veterinary Medicine, Yangzhou University, Yangzhou, 225009, China
[c] Jiangsu Co-innovation Center for Prevention and Control of Important Animal Infectious Diseases and Zoonosis, Yangzhou University, Yangzhou, 225009, China
[d] Jiangsu Key Laboratory of Zoonosis, Yangzhou, 225009, China
[e] Institute of Translational Medicine, Key Laboratory of Geriatric Disease Prevention and Control of Jiangsu Province, Medical College, Yangzhou University, Yangzhou, 225009, China

ARTICLE INFO

Keywords:
H9N2
Hemagglutinin (HA)
PB2-627K
Mammalian adaptation
Pathogenicity
Transmissibility

ABSTRACT

H9N2 avian influenza viruses (AIVs) circulate globally in poultry and have become the dominant AIV subtype in China in recent years. Previously, we demonstrated that the H9N2 virus (A/chicken/Eastern China/SDKD1/2015) naturally harbors a mammalian-adaptive molecular factor (627K) in the PB2 protein and is weakly pathogenic in mice. Here, we focused on new markers for virulence in mammals. A mouse-adapted H9N2 virus was serially passaged in mice by infecting their lungs. As expected, infected mice showed clinical symptoms and died at passage six. A comparison between the wild-type and mouse-adapted virus sequences identified amino acid substitutions in the hemagglutinin (HA) protein. H9N2 viruses with the T187P + M227L double mutation exhibited an increased affinity to human-type (SAα2,6Gal) receptors and significantly enhanced viral attachment to mouse lung tissues, which contributed to enhancing viral replication and virulence in mice. Additionally, HA with the T187P + M227L mutation enabled H9N2 viral transmission in guinea pigs via direct contact. AIV pathogenicity in mice is a polygenic trait. Our results demonstrated that these HA mutations might be combined with PB2-627K to significantly increase H9N2 virulence in mice, and this enhanced virulence was achieved in other H9N2 AIVs by generating the same combination of mutations. In summary, our study identified novel key elements in the HA protein that are required for H9N2 pathogenicity in mice and provided valuable insights into pandemic preparedness against emerging H9N2 strains.

1. Introduction

H9N2 avian influenza viruses (AIVs) affect poultry worldwide. In 1966, this influenza A virus subtype was originally isolated from turkeys in the United States (Homme and Easterday, 1970) and over the following decades, migratory birds spread it to Eurasia, Middle East and Africa (Alexander, 2003). During the 1990s, H9N2 AIVs, which were initially isolated from chickens in southern China, became prevalent in poultry (Guan et al., 1999; Pu et al., 2015). Typically, they cause mild clinical signs in poultry, such as respiratory disorders, reduced egg production, and decreased body weight, resulting in significant economic losses.

H9N2 AIVs pose great challenges to both poultry production and public health. H9N2 AIVs can increase the viral pathogenicity and infectivity of the novel reassortant H7N9, H5N6, H10N8 and H10N3 subtypes in humans by contributing whole sets of internal genes (Chen et al., 2013, 2014; Shen et al., 2016; Liu et al., 2022). H9N2 AIVs are also a potential threat to public health because they can cross the species barrier even infecting humans. In 1999, the first human case was confirmed in Hong Kong (Peiris et al., 1999), and in subsequent surveillance, cross-species transmissions of H9N2 AIVs have occasionally been reported in Chinese mainland, Egypt, Bangladesh, Pakistan, and Oman (Peacock et al., 2019). There has been a significant increase in laboratory-confirmed human H9N2 infections in recent years, with a total of 57 reported cases to WHO since December 2015 and 16 cases in 2021 (WHO, 2022). Most human infections are only associated with mild clinical symptoms except for one reported death of a 57-year-old woman who was infected with

* Corresponding authors.
E-mail addresses: wxq@yzu.edu.cn (X. Wang), xfliu@yzu.edu.cn (X. Liu).

https://doi.org/10.1016/j.virs.2022.09.006
Received 1 April 2022; Accepted 7 September 2022
Available online 11 September 2022

H9N2 but also had underlying health conditions (Peacock et al., 2019). Additionally, most human infection cases were exposed to H9N2 AIV through contact with infected poultry or environmental contamination, and no case clusters have been reported (WHO, 2022). In addition to the diagnosis of H9N2 viral infection, extensive serological evidence has shown poultry workers with high seropositivity rates among many enzootic countries (Khan et al., 2015). In summary, cross-species transmissions of H9N2 AIVs from poultry to humans occur frequently, but this influenza A virus subtype usually results in mild or no symptoms and unsustainable human-to-human transmission. This suggests that H9N2 can infect humans across interspecies barriers, but there are other factors that limit the virulence to humans.

An epidemiological survey on AIV in China between 2014 and 2016 determined that H9N2 was the dominant subtype in northern China at that time (Bi et al., 2016; Liu et al., 2020). The 2016–2019 survey showed that positivity rates had substantially declined for other AIVs but increased annually for H9N2 AIV, which dominates in Chinese mainland (Bi et al., 2020; Guo et al., 2021; Liu et al., 2020). More importantly, H9N2 has become the most prevalent subtype in ducks and chickens, which increases the potential for reassortment with other AIV subtypes (Bi et al., 2020). Thus, H9N2 circulation has become highly complex in China. The high H9N2 positivity rates imply that the virus will have more opportunities to infect humans, especially if it acquires effective human receptor-binding capacity (Bi et al., 2020).

During our AIV surveillance of live-bird markets in eastern China, we isolated one H9N2 strain A/chicken/Eastern China/SDKD1/2015 (SDKD1) that naturally harbored molecular factors for adaption to mammals in the hemagglutinin (HA; 226L and 228S) and PB2 (627K) proteins (Liu et al., 2021), indicating that H9N2 had acquired the ability to adapt to mammals. Although SDKD1 can bind to human receptor analogs (SAα-2,6-Gal) and prompt viral replication in mammalian cells, it is weakly pathogenic in mice (Liu et al., 2021). To identify other key virulence markers of the H9N2 virus in mammals, we performed a serial-passaging experiment using the SDKD1 strain in mice. Our results suggested that amino acid substitutions in both the HA protein and PB2-627K contributed to H9N2 virulence in mice.

2. Materials and methods

2.1. Viruses and cell lines

The H9N2-subtype AIVs, A/chicken/Eastern China/SDKD1/2015 and A/chicken/Eastern China/AH320/2015, were obtained from chickens that appeared to be in good health in eastern China and reserved in our laboratory (Liu et al., 2021). Nucleotide sequences of SDKD1 and AH320 were available from Global Initiative on Sharing all Influenza Data (https://platform.gisaid.org, GISAID) under accession numbers EPI1800491 to EPI1800498 and EPI2080949 to EPI2080956, respectively. The viruses were amplified in 9-day-old specific-pathogen-free (SPF) embryonated eggs (Merial, China) and properly stored at −80 °C. Primary chicken embryo fibroblasts (CEFs) were prepared in our lab. Human embryonic kidney (293T), Madin-Darby canine kidney (MDCK), and human lung carcinoma (A549) cells were grown in Dulbecco's modified Eagle's medium (DMEM; Invitrogen, USA) with 10% fetal bovine serum (FBS; Gibco, New Zealand).

2.2. Passaging of H9N2 AIV in BALB/c mice

The mouse-adapted H9N2 variants were generated by serial mouse lung-to-lung passages, as described previously (Li et al., 2014b). Briefly, 6-week-old BALB/c mice were lightly anesthetized with pentobarbital sodium and intranasally infected with 50 μL of $10^{6.0}$ 50% egg infectious dose (EID_{50}) of wild-type H9N2 (SDKD1). After 3 days post-inoculation (dpi), lungs of infected mice were collected, homogenized, and centrifuged. Supernatant aliquots (50 μL) were collected and used to inoculate naïve mice for subsequent passages. After six passages, viruses from the lung homogenates of every passage were amplified in chicken embryos. Passage-six (SDKD1-P6) viruses were purified in MDCK cells for three rounds, as documented previously (Hayden et al., 1980).

2.3. Sequence analysis

Viral RNA was extracted for PCR amplification by using the commercial kit (TransGen, China). Two-step reverse transcription PCR was carried out as described previously (Hoffmann et al., 2001). Then Sanger sequencing was performed on the purified PCR products. Full amino acid sequences of SDKD1-P6 virus were aligned with those of the SDKD1-WT virus using MEGA 7 (Sinauer Associates, Inc., USA).

2.4. Plasmid construction and viral rescue

All gene segments of A/chicken/Eastern China/SDKD1/2015 and A/chicken/Eastern China/AH320/2015 were cloned into the pHW2000 vector, as previously described (Hoffmann et al., 2000). Mutations in the *HA* gene (T187P, M227L, T187P + M227L) and *PB2* gene (K627E) of the SDKD1-WT virus, along with mutations in the *HA* gene (T187P + M227L) and *PB2* gene (E627K) of the AH320-WT virus, were generated using the Fast Mutagenesis System kit (TransGene, China). Eight plasmids were co-transfected into 293T cells using the Lipofectamine 2000 Reagent (Invitrogen, USA). Culture supernatant aliquots were harvested at 72 h post-transfection, and 9-day-old chicken embryos were infected and incubated for 96 h. Parental and mutant viruses were purified for three rounds and confirmed by sequencing. Aliquots of viral fluid were stored at −80 °C.

2.5. Mouse pathogenicity experiments

BALB/c mice (female, 6 weeks old), were provided by the Yangzhou Experimental Animal Center (China). The mice (n = 5, per group) intranasally inoculated with 50 μL of $10^{3.0}$–$10^{7.0}$ EID_{50} of each virus strain diluted in sterile phosphate-buffered saline (PBS) after anesthesia. Changes in body weight and mortality among the mice were recorded over the following 14 days, and humane euthanasia was used for mice that had lost 25% or more of their original weight. The Reed and Muench method was used to calculate the 50% mouse lethal dose (MLD_{50}) (Reed and Muench, 1938). To examine viral distribution in the respiratory system, three mice were inoculated with $10^{6.0}$ EID_{50} of the virus and euthanized at 1, 3, and 5 dpi. Mouse lungs, tracheas, and nasal turbinates were collected and homogenized in 1.0 mL of PBS used for determining viral titers by performing the EID_{50} assay. A portion of lungs (left, 30%) from each mouse group at 3 dpi was collected for histopathological examination.

2.6. Guinea pig transmissibility experiments

The method used in this part has been previously described in detail (Liu et al., 2022). Briefly, nine guinea pigs (Vital River Laboratories, China) were divided into three equal groups, infection, contact and aerosol group, respectively. The route of transmission is determined by measuring the virus titer from the collected nasal wash and seroconversion rates among all animals.

2.7. Growth dynamics of mutant virus in different cell lines

To evaluate the growth dynamics *in vitro*, MDCK, A549, and CEF cells were infected with selected viruses at a multiplicity of infection (MOI) of 0.001 50% tissue culture infectious dose ($TCID_{50}$). Each test was performed in triplicate, and samples were incubated at 37 °C. Following 8, 12, 24, 36, 48, and 60 h post-infection (hpi), supernatants were harvested. Viral titers were expressed as the $TCID_{50}$/mL in MDCK cells.

2.8. Receptor-binding specificity assay

Viral receptor affinity was evaluated by a solid-phase binding assay, as described previously (Li et al., 2014a). Briefly, two biotinylated chemically synthesized trisaccharides, including avian receptor analogs (3′SLN) and human receptor analogs (6′SLN) (GlycoTech, USA), were added to wells following gradient concentrations and bound to 96-well streptavidin-coated microtiter plates (Thermo Fisher, USA). PBS with 2% skim milk powder was used for blocking the microtiter plates, and 128 HA units of live virus were added to each well. The plates were incubated with chicken antiserum obtained for each virus and subsequently with horseradish peroxidase-conjugated rabbit anti-chicken IgG antibody (Sigma, USA). Aliquots of 1 mol/L H_2SO_4 were added after TMB reagent, and the absorbance was measured at 450 nm. Each sample was measured in triplicate.

2.9. Virus binding to cells and tissues

A549 and CEF cells in 96-well-plates were incubated with 64 HA units of wild type (WT) or mutant viruses at 4 °C for 1 h. Then, cells were washed thrice in cold PBS and fixed for 1 h in 4% paraformaldehyde. The washing step with cold PBS was repeated thrice to prepare cells for the incubation with the corresponding chicken antiserum at a 1:500 dilution (1 h at 4 °C). The washing step with cold PBS was again repeated thrice, and cells were incubated for 1 h at 4 °C before adding a 1:1000 dilution of the secondary antibody (anti-chicken IgG conjugated with FITC; Life Technologies, USA). Cells were again washed thrice with cold PBS, and the nuclei were stained with DAPI dye (Beyotime Biotechnology, China) for 10 min at 37 °C, and observed under a fluorescence microscope (Nikon). The preparation of tissue sections has been described detailedly in our previous research article (Liu et al., 2022). The following steps were similar with the procedure described in virus binding to cells.

2.10. Determination of plaque morphology

After washing monolayers of MDCK cells in 6-well dishes twice with PBS, a serial dilution of the virus was seeded per well. Incubated for 1.5 h, cells were washed twice with PBS followed by covering with DMEM containing 0.8% agar (Sigma, St. Louis, MO, USA) and 2% FBS. After incubation for 72 h in 5% CO_2 at 37 °C, fixed cells were stained with a formaldehyde solution containing 1% crystal violet, and observed for plaque morphology. Plaque size was measured using Image Pro-Plus, version 6.0 (Media Cybernetics, USA), and as many as possible of plaques were conducted to ensure the accuracy. The plaque size of the mutant viruses was indicated as x-fold increase compared to the wild type virus.

3. Results

3.1. Derived mouse-adapted H9N2 viruses

In previous studies, the H9N2 isolate SDKD1-WT displayed weak pathogenicity in mice, suggesting human adaption mutations in HA (Q226L, G228S) and PB2 (E627K) were insufficient to enhance the virulence of this strain in mammals. In the present study, the SDKD1-WT isolate was serially passaged in mice to increase its virulence. As expected, infected mice showed clinical symptoms and died at passage six, the MLD_{50} value was 3.6 $\log_{10}$ EID_{50}. Thus, we successfully derived a mouse-adapted variant SDKD1-P6.

3.2. Mapping the crucial HA mutation sites required for increasing the H9N2 AIV pathogenicity in mice

Whole genome sequencing of SDKD1-WT and SDKD1-P6 was performed to identify the adaptive mutations correlated with the increased virulence in mice. An alignment of the full coding sequences of SDKD1-WT and SDKD1-P6 identified two amino acid substitutions (T187P and M227L) and a deletion of three consecutive amino acids (Δ222–224) in the HA protein. No other proteins had amino acid mutations.

Next, we generated a series of mutant viruses by reverse genetics to identify amino acid mutations that contributed to the pathogenicity of the mouse-adapted variant in mice. We used SDKD1-WT as the backbone to generate rSDKD1-WT and four mutant viruses: rSDKD1-T187P, rSDKD1-M227L, rSDKD1-T187P+M227L and rSDKD1-P6 (three consecutive amino acids deletion, Δ222–224, was not common in nature, so we did not study it). We assessed the virulence by intranasally inoculating groups of mice (n = 5) each with $10^{3.0}$–$10^{7.0}$ EID_{50} of rSDKD1-WT, rSDKD1-T187P, rSDKD1-M227L, rSDKD1-T187P+M227L or rSDKD1-P6, which was followed by a 2-week observation period. The corresponding MLD_{50} values were as follows: rSDKD1-WT, > 7.5 $\log_{10}$ EID_{50}; rSDKD1-T187P, > 7.5 $\log_{10}$ EID_{50}; rSDKD1-M227L, > 7.5 $\log_{10}$ EID_{50}; rSDKD1-T187P+M227L, 4.4 $\log_{10}$ EID_{50}; rSDKD1-P6, 3.6 $\log_{10}$ EID_{50} (Fig. 1). Thus, the T187P + M227L double mutations in HA were the key markers to enhanced the virulence of H9N2 in mice.

We performed a histopathology analysis of lung tissues recovered from normal mice and infected mice at 3 dpi. In comparison with lung tissues from control group, no pathological damage in lungs of the rSDKD1-WT group existed (Fig. 2A). However, infections by the rSDKD1-T187P+M227L was associated with more severe characteristics, including localized bronchointerstitial pneumonia, bronchial lumen erythrocyte infiltration, and interstitial widening, which displayed occasional foci of necrosis of bronchial and bronchiolar epithelial cells, multifocal hemorrhaging, and inflammatory cell infiltration (Fig. 2A).

To further investigate mechanisms contributing to the increased pathogenicity in mice, we quantified replication capacities of WT and mutant viruses in mouse respiratory tissues (lung, turbinates, and trachea) at different infection stages. Three mice from the rSDKD1-WT and rSDKD1-T187P+M227L ($10^{6.0}$ EID_{50}) groups were euthanized at 1, 3, and 5 dpi, and respiratory tissues were collected to determine viral titers. Consistent with the body weight loss results, higher viral titers were observed in lungs and tracheas from the mice infected with mutant viruses, compared to those inoculated with the WT virus (Fig. 2B). However, viral replication in the nasal turbinates did not significantly vary between the WT and mutant viruses (Fig. 2B). Thus, the elevated virulence of certain mutant viruses in our study might result from an increased viral replication in the respiratory system.

3.3. Growth dynamics of mutant virus in different cell lines

To emulate host-switching events *in vitro*, replication ability of the pathogenicity-associated mutant viruses were tested in different host cells. MDCK, A549 and CEF cells were inoculated with viruses at an MOI of 0.001, to quantify the viral replication dynamics during an overt infection (8–60 hpi). In mammalian cells (MDCK and A549), viruses carrying pathogenicity-associated mutation generated significantly higher titers than the rSDKD1-WT virus during the initial infection stages (8 and 12 hpi), whereas the viral titers did not significantly differ during the middle and late infection stages (Fig. 3). Additionally, the viral growth kinetics did not differ in the avian-derived CEF cells (Fig. 3). These results indicated that the pathogenicity-associated HA mutations primarily increased the viral replication ability in mammalian cell lines during the initial infection stages.

3.4. Transmission of the of mutant virus in Guinea pigs

To assess the role of the amino acid mutations in HA in spreading the H9N2 AIVs among mammals, we examined the transmission of these viruses by infecting naïve guinea pigs via direct contact and respiratory droplets. In the rSDKD1-WT groups, viruses were only isolated from inoculated animals, and neither the virus from the nasal washes, nor H9N2 seroconversion was detected among the contact or aerosol groups, indicating the absence of horizontal transmission during the 21-day infection period (Fig. 4). However, the rSDKD1-T187P+M227L virus

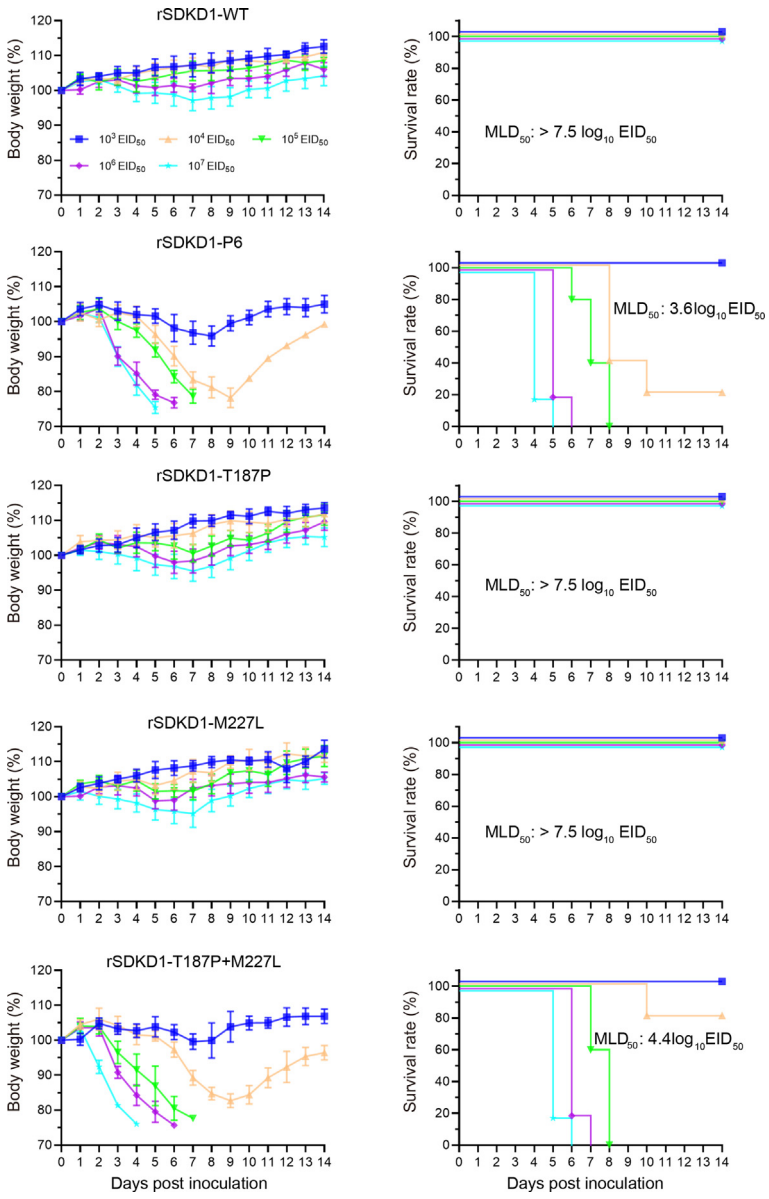

Fig. 1. Mapping of crucial mutation sites in HA protein that increased H9N2 AIVs virulence in mice. Five six-week-old female BALB/c mice per group were inoculated intranasally with 50 μL of PBS containing $10^{3.0}$–$10^{7.0}$ EID$_{50}$ of mutated viruses. Body weight and survival were monitored daily for 14 dpi. The body weights of each group were shown as mean with standard deviation. Mice were humanly sacrificed when losing ≥ 25% of the initial body weight.

were transmitted to one direct contact guinea pig (Fig. 4, Table 1). These findings demonstrated that mutant virus did not acquire the ability to spread via respiratory droplets, but the T187P + M227L double mutation combined with PB2-627K enabled H9N2 viral transmissibility among guinea pigs via direct contact.

3.5. Mutant virus had increased affinity for human-type receptors

One natural barrier preventing AIV adaptation in mammals is the difference between avian and human receptor types. We initially evaluated receptor-binding preference of the rescued WT and mutant viruses. The control viruses of A/California/04/2009 [H1N1 (CA04)] and A/mallard/Huadong/S/2005 [H5N1 (HD05)] showed an absolute preference for human-type (SAα-2,6 Gal) and avian-type (SAα-2,3 Gal), respectively (Supplementary Fig. S1). The rSDKD1-WT and rSDKD1-T187P + M227L could bind to both the avian-type (SAα2,3Gal) and human-type (SAα2,6Gal) receptors (Fig. 5A). However, the rSDKD1-T187P+M227L virus had a lower affinity to SAα2,3Gal and a higher affinity to SAα2,6Gal than the rSDKD1-WT virus, indicated that these HA mutations increased the viral affinity to human-type receptors.

Because many of the glycan structure components presenting on the SAα2,3Gal and SAα2,6Gal receptors were unavailable in synthetic substrates, affinities of the WT and mutant virus for different receptors were directly tested on mammalian and avian cells and tissues (Walther et al., 2013; Ning et al., 2009). We measured the fluorescence intensity after incubating the viruses with A549 and CEF cells for 1 h. The incubation with rSDKD1-T187P+M227L generated significantly higher fluorescence intensities in A549 cells than the incubation with rSDKD1-WT (Fig. 5B and C), indicated that these HA mutations increased the ability of the virus to bind to human-derived A549 cells but not to avian-derived CEF cells.

We also examined the host tissue tropism of the rescued WT and mutant virus by incubating them with mouse lung and duck intestinal tract tissue sections. The former displays mainly SAα2,6Gal receptors (Ning et al., 2009; Teng et al., 2016), but the latter contains various glycan receptors with SAα2,3Gal as terminal receptor components (Song et al., 2017). Consistent with the viral binding test results in cells from different

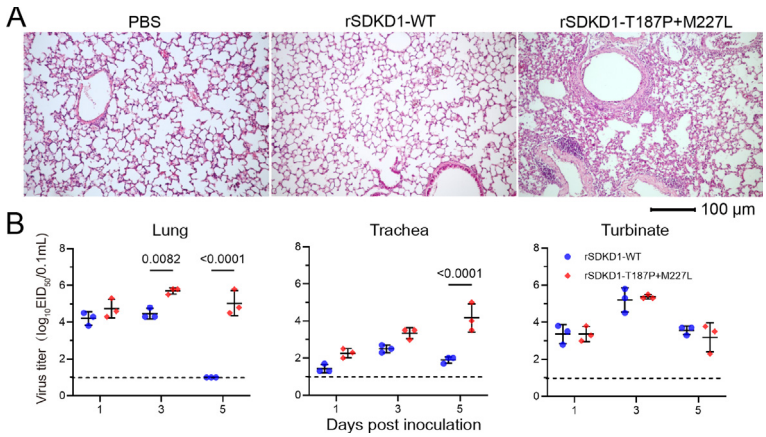

Fig. 2. T187P + M227L double mutations in HA enhanced H9N2 virulence *in vivo*. **A** Histopathology of the lungs of mice inoculated with wild-type (WT) and mutant virus. At 3 dpi, lungs were collected from mice inoculated with $10^{6.0}$ EID_{50} of WT and mutant viruses, and were fixed with formalin, embedded in paraffin and stained with hematoxylin and eosin. The images were obtained at a magnification of × 20. Scale bar = 100 μm. **B** Replication of the WT and mutant virus in respiratory system of infected mice. Three mice inoculated with $10^{6.0}$ EID_{50} of desired viruses were euthanized on 1, 3 and 5 dpi. Lung, trachea and nasal turbinate were collected and homogenized in 1.0 mL of PBS. Virus titers were determined by performing EID_{50} assay per 0.1 mL in 9-days-old SPF chicken embryos. The values are expressed as means with standard deviations. Statistical analysis was performed by GraphPad software, and statistical significance was assessed by using the two-tailed unpaired Student's *t*-test.

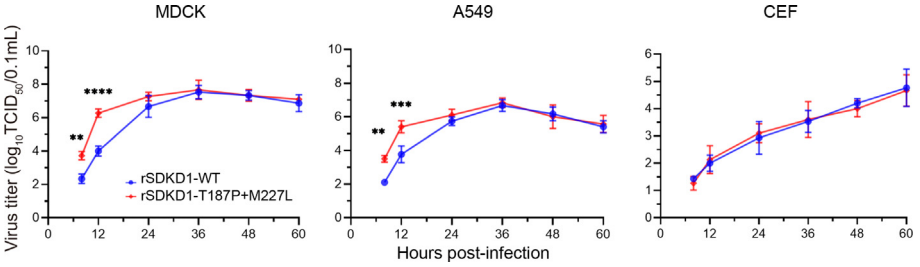

Fig. 3. Growth dynamics of wild type (WT) and mutant virus in different cell lines. MDCK, A549, and CEF were inoculated with the indicated viruses at a multiplicity of infection (MOI) of 0.001 $TCID_{50}$/cell in triplicate at 37 °C. Supernatants were aseptically harvested at 8, 12, 24, 36, 48, and 60 hpi. The virus titers were determined by performing $TCID_{50}$ per 0.1 mL in MDCK cells. Statistical analysis was performed by GraphPad software, and statistical significance was assessed by using the two-tailed unpaired Student's *t*-test. $^{**}P < 0.01$, $^{***}P < 0.001$, $^{****}P < 0.0001$.

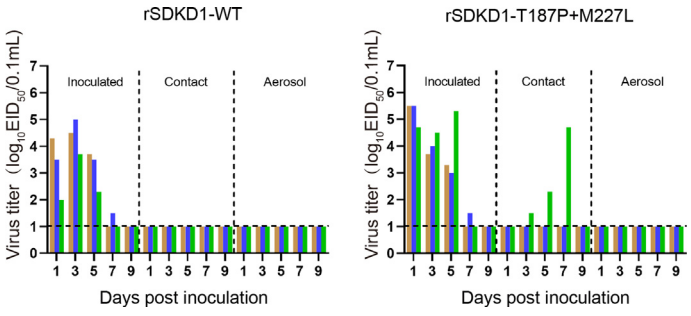

Fig. 4. Horizontal transmissions of wild type (WT) and mutant virus in guinea pigs. Groups of guinea pigs seronegative for influenza viruses (n = 3) were inoculated with $10^{6.0}$ EID_{50} of the indicated viruses. On the next day, the three inoculated guinea pigs were individually paired by co-housing with a direct-contact guinea pig. In addition, three aerosol contact guinea pigs were housed in a wire frame cage adjacent to that of the infected guinea pig. The distance between the cages of the infected and aerosol-contact guinea pigs was 5 cm apart. Nasal washes were collected from all animals for virus shedding detection every other day beginning on day 1 after the initial infection. Virus titers were determined by EID_{50} assay per 0.1 mL in 9-days-old SPF chicken embryos. Each color bar represents the virus titer in an individual animal.

species, HA mutations increased the viral binding ability to mouse lung tissue but not to the duck intestinal tract sections (Fig. 5B and C). These results indicated that T187P + M227L combined mutation in HA protein increased the binding affinity of the virus to human-type receptors.

3.6. Mutant virus formed large plaques in MDCK cell monolayers

We assessed the replication of the parental WT and mutant virus by comparing their ability of plaque formation in MDCK cell monolayers. rSDKD1-T187P+M227L formed larger plaques than the parental rSDKD1-WT (Fig. 6). The plaque size associated with the HA mutants were heterogeneous, which probably caused by the use of non-synchronized cells for infection instead of mixed viral populations. Therefore, HA mutations were associated with the changed plaque morphology, and these HA mutants promoted the replication ability, compared to the WT virus.

3.7. The combination of HA mutant variant with PB2 627E did not enhance H9N2 pathogenicity in mice

AIV polymerases have been confirmed to play a role in mammalian adaption, especially the PB2 E627K substitution (Liu et al., 2019; Hatta et al., 2001; Linster et al., 2014; Mok et al., 2014; Shi et al., 2017; Zhang et al., 2013). The PB2 E627K substitution enhances viral polymerase activity, which promotes viral replication and increases pathogenicity. To

Table 1
Seroconversion of guinea pigs.

Strains	Seroconversion: no. positive/no. total (HI titers, log2)[a]		
	Inoculated	Direct contact	Aerosol
rSDKD1-WT	3/3 (7, 6, 7)	0/3	0/3
rSDKD1-T187P+M227L	3/3 (7, 7, 5)	1/3 (4)	0/3

[a] Sera were collected from guinea pigs on 21 days post inoculation and treated with receptor destroying enzyme (RDE). Seroconversion was confirmed by HI assay.

explore the effect of HA mutations on viral virulence in the presence of PB2 627E, we rescued the rSDKD1-WT-K627E and rSDKD1-T187P+M227L+K627E mutant variants. We inoculated five BALB/c mice per group with $10^{6.0}$ EID_{50} of the indicated virus variants (Fig. 7). No mice died during the post-infection period, indicating that these virus variants were only weakly pathogenic in mice (MLD_{50} > 6.5 log_{10} EID_{50}). Thus, as described above, the combination of the HA mutations (T187P+M227L) with PB2-627K was critical for the virulence in mice.

3.8. The combination of HA mutation with PB2 627K enhanced the pathogenicity of other H9N2 strains in mice

As described above, the H9N2 virus, SDKD1, naturally harbors mammalian-adaptive molecular factors (PB2-627K) that combined with HA protein mutations (T187P+M227L) and can enhance pathogenicity in mice. In this study, we tested whether gaining these HA mutations also affected the pathogenicity of other H9N2 viruses. We used the A/chicken/Eastern China/AH320/2015 (AH320) (Supplementary Table S1) backbone to construct reverse-genetic variants with HA mutations combined with PB2-E627K. The AH320 strain has the avian molecular marker, E residue at 627 aa in PB2. Five BALB/c mice per group were inoculated with $10^{6.0}$ EID_{50} of viruses only carrying HA mutations (rAH320-T187P+M227L), and no mice died during the post-infection period, indicating weak pathogenicity of these viruses in mice (MLD_{50} > 6.5 log_{10} EID_{50}; Fig. 8). However, virus variants containing these HA mutations combined with PB2-627K (rAH320-T187P+M227L+E627K) had significantly higher pathogenicity in the mice than those in the rAH320-E627K variant. This result supported our observations with the SDKD1 virus and illustrated that the combination of HA mutants and PB2-627K could enhance the pathogenicity in other H9N2 virus variants as well.

3.9. Prevalence of amino acid type at positions 187 and 227 of HA protein in H9N2 viruses

In order to determine the prevalence of amino type of HA-187 and HA-227 in different host-derived H9N2 viruses, available H9N2 HA sequences were downloaded from the GISAID database. As shown in Table 2, HA-187T accounted for 98.39%, 100% and 100% of the avian-derived, human-derived, and swine-derived H9N2 strains, respectively. HA-187P was not discovered in natural H9N2 strains. Amino acid diversity was founded in position HA-227. As shown in Table 2, the proportion of HA-227M (40.72%) and 227Q (40.44%) were approximately close in avian-derived H9N2 strains. In addition, HA-227M was predominant in human-derived (64.41%) strains and 227Q was predominant in swine-derived (62.50%) strains. Although HA-227L was present in natural H9N2 strains, the proportion (0.08%) was extremely low. These data indicate that HA-T187P and M227L may pose a lower threat to current global public health security.

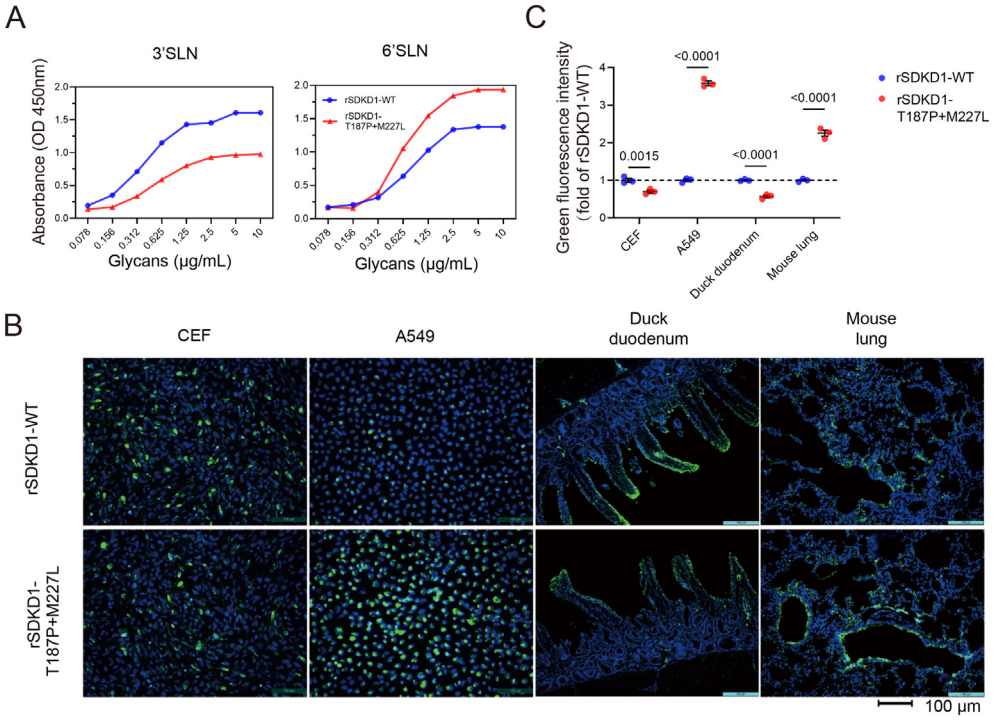

Fig. 5. Receptor binding properties of wild type (WT) and mutant virus. **A** Solid-phase receptor-binding assay. Direct binding of viruses to sialyl glycopolymers containing either 3′SLN-PAA or 6′SLN-PAA was measured. The mean data shown are representative of three independent binding experiments. **B** Binding of WT and mutant viruses to different host origin cell lines, duck duodenum and mouse lung tissues. Cells and tissues were incubated with each H9N2 virus and subsequently incubated with an anti-H9N2 polyclonal antibody and an FITC-labeled secondary antibody and DAPI dye (blue), then observed under a fluorescence microscope. Green staining indicated that virus binding occurred. Experiments were performed three times, with representative images shown here. Scale bar = 100 μm. **C** Fold change of green fluorescence intensity of mutant virus to WT in (**B**) was calculated. Statistical analysis was performed by GraphPad software, and statistical significance was assessed by using the two-tailed unpaired Student's *t*-test.

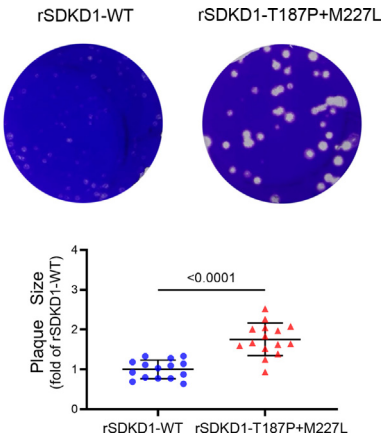

Fig. 6. Plaque-forming ability of wild type (WT) and mutant virus in MDCK cells. For the detection of plaque-forming ability, MDCK monolayer cells were infected with each H9N2 viruses, covered with an agarose-containing overlay for 72 h and stained with crystal violet. The plaque size of the mutant viruses was indicated as x-fold increase compared to the WT virus. Experiments were performed three times, with representative images shown here. Statistical analysis was performed by GraphPad software, and statistical significance was assessed by using the two-tailed unpaired Student's *t*-test.

4. Discussion

H9N2 AIV circulates globally in poultry and has become the dominant AIV subtype in China in recent years (Bi et al., 2020; Guo et al., 2021). H9N2 has a significant negative impact on the poultry industry, causing economic losses. Human H9N2 infections have significantly increased since 2015, and H9N2 seroprevalence in poultry workers remains high (Khan et al., 2015; Hoa et al., 2017), indicating that H9N2 AIV is also a public health threat.

The adaptation of AIVs to mammalian hosts requires overcoming some species-specific barriers in receptor binding and polymerase activity (Taubenberger and Kash, 2010; Ciminski et al., 2021; Long et al., 2019; Bisset and Hoyne, 2020). The switch to human-type receptors is a prerequisite for H9N2 AIVs to transmit efficiently in mammals (Thompson and Paulson, 2021; Sun et al., 2020; Shinya et al., 2006; Peacock et al., 2020). Interestingly, most H9N2 viruses circulating in China have a high affinity for human-type receptors (Bi et al., 2020; Li et al., 2014c), which is similar to that observed for human influenza viruses (Ciminski et al., 2021; Matrosovich et al., 2000). As one of the two types of viral surface glycoproteins, HA plays a critical role in overcoming receptor-binding restrictions (de Vries et al., 2017a, 2017b; Van Hoeven et al., 2009; Song et al., 2017). Here, we demonstrated that amino acid mutations (T187P + M227L) in HA could enhance the ability of the H9N2 virus to bind to human-type receptors. Homology modeling results (data not shown) indicated that the HA 187 aa residue was located near the 190-helix, and the 227 aa residue was located in 220-loop of the receptor-binding site (RBS). The RBS of the HA protein is critical for AIV host range restriction (Stevens et al., 2006; Shi et al., 2014; Kong et al., 2021). Our results highlighted that the newly identified mutations (T187P + M227L) were required for enhancing the viral affinity to SAα2, 6Gal, and they appeared to be the most important factor for the increased viral replication in mammalian cells at the early infection stages, along with the ability to form larger plaques in MDCK cell monolayers and to increase the pathogenicity in mice.

We previously showed that the SDKD1-WT virus could be transmitted from chicken to chicken and from chicken to guinea pig via respiratory droplets (Liu et al., 2021). However, a pandemic H9N2 AIV variant can only emerge if it acquires the ability of continuous transmission between humans, similar to the H1 and H3 viral strains (Watanabe et al., 2014). In this study, T187P + M227L double mutations combined with PB2-627K were critical for mediating direct-contact transmission. However, without other factors, newly identified mutations were insufficient for respiratory droplet transmission in mammals, despite the high titers in the nasal washes. Therefore, H9N2 needs to acquire more adaptive substitutions to achieve effective transmission rates in mammals.

The pathogenicity of AIV in mice is a polygenic trait (Neumann and Kawaoka, 2006; Watanabe et al., 2014; Hao et al., 2019; Kong et al., 2019). Aside from the receptor-binding affinity conferred by HA, the polymerase also functions as a virulence determinant (Song et al., 2014; Ma et al., 2020; Mok et al., 2014; Liang et al., 2019; Klumpp et al., 1997). During AIV replication, HA enhances cell tropism and mediates the binding of the viruses to host cells (Long et al., 2019; Mair et al., 2014). Subsequently, PB2 is required to optimize replication after entering targeted cells (Song et al., 2014; Arai et al., 2019). Several studies have reported that avian-derived AIVs also have the mammalian-adaptive substitution E627K in the PB2 protein (Gu et al., 2020; Ge et al., 2018), indicating that several subtype AIVs are evolving to adapt to mammals. SDKD1-WT naturally harbors the E627K substitution in PB2, but this strain remains to be lowly pathogenic in mice (Liu et al., 2021). Rescued H9N2 viruse containing PB2-627E and the HA combined mutation (T187P+M227L) was weakly pathogenic in mice. We found that combinations of PB2-627K with these HA mutations were related to increased virulence in mice. Remarkably, the combination of these HA mutations and PB2-627K contributed to the pathogenicity of the SDKD1-WT virus and other H9N2 strain in mice as well, which excluded strain specificity as a requirement for effective pathogenicity.

5. Conclusions

In summary, our findings demonstrated that the H9N2 virus, which naturally harbors PB2-627K, required other adaptive substitutions in the HA protein to cross species barriers and enhance the viral virulence phenotype in mice. We identified viruses with distinct HA mutations that exhibited an increased affinity to human-type (SAα2,6Gal) receptors and

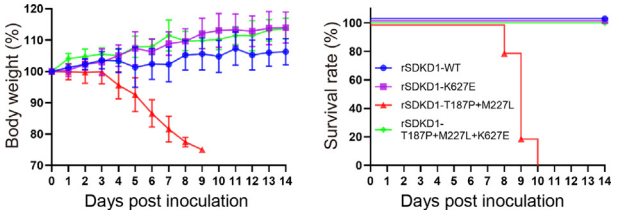

Fig. 7. HA mutations combined with PB2-627K enhance pathogenicity of the H9N2 virus in mice. Five six-week-old female BALB/c mice per group were inoculated intranasally with 50 μL of PBS containing $10^{6.0}$ EID_{50} of each virus. Body weight and survival were monitored daily for 14 dpi. The body weight of each group were shown as mean with standard deviation. Mice were humanly sacrificed when losing ≥ 25% of the initial body weight.

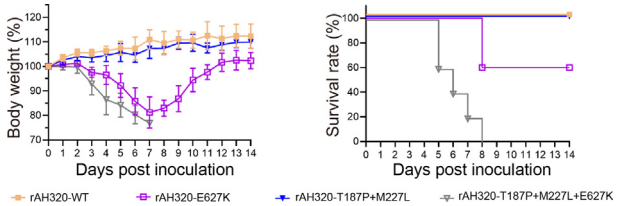

Fig. 8. The effect that HA mutation combined with PB2627K can enhance the pathogenicity in mice also works in other H9N2 strains. A series of recombinant viruses were constructed based on A/chicken/Eastern China/AH320/2015 (H9N2) backbone. This strain possesses the avian molecular marker E at 627 aa position in PB2 protein. Five six-week-old female BALB/c mice per group were inoculated intranasally with 50 μL of PBS containing $10^{6.0}$ EID_{50} of indicated viruses. Body weight and survival were monitored daily for 14 dpi. The body weight of each group were shown as mean with standard deviation. Mice were humanly sacrificed when losing ≥ 25% of the initial body weight.

Table 2
Prevalence of amino acid type at positions 187 and 227 of HA protein in H9N2 viruses.

Position[a]	Host species[b]						
	Amino	Avian		Human		Swine	
	acid	Count	Relative frequency (%)	Count	Relative frequency (%)	Count	Relative frequency (%)
187	T	2445	98.39	59	100	72	100
	A	28	1.13	0	0	0	0
	P	0	0	0	0	0	0
	Others	12	0.48	0	0	0	0
227	M	1012	40.72	38	64.41	1	1.39
	Q	1005	40.44	17	28.81	45	62.50
	I	442	17.79	4	6.78	0	0
	L	2	0.08	0	0	0	0
	H	0	0	0	0	26	36.11
	Others	24	0.97	0	0	0	0
Total		2485	100	59	100	72	100

[a] H3 numbering.
[b] The H9 protein sequences were downloaded from the GISAID database. Duplicate, gapped, or truncated sequences were excluded prior to analysis.

a significantly enhanced viral attachment to mouse lung tissues, which was associated with an increased viral replication and virulence in mice. Thus, our findings suggested that HA mutations T187P + M227L synergized with PB2-E627K might promote H9N2 AIVs to cross species barriers. Our study identified novel critical changes in the H9N2 surface proteins, which facilitated the virulence in mice. Thankfully, T187P and M227L mutations were not yet prevalent in current H9N2 strains. Nevertheless, our study will provide early warning of pandemic caused by potentially evolved H9N2 strains in future.

Data availability

The data supporting the findings of this study are available from the corresponding author.

Ethics statement

All experiments involving animals were carried out as Animal Welfare guidelines directed and approved by the Jiangsu Administrative Committee for Laboratory Animals (SYXK-SU-2017-0044 and SYXK-SU-2016-0019). All experiments with live virulent H9N2 viruses and animals were performed under animal biosafety level-3 (ABSL-3) conditions according to the institutional biosafety procedures.

Author contributions

Kaituo Liu: conceptualization, investigation, methodology, validation, writing - original draft preparation, visualization. Yaqian Guo: investigation, methodology, validation, formal analysis. Huafen Zheng: investigation, methodology. Zhuxing Ji: investigation, methodology. Miao Cai: investigation, methodology. Ruyi Gao: formal analysis, data curation, validation. Pinghu Zhang: formal analysis, data curation, validation. Xiaowen Liu: formal analysis, data curation, validation. Xiulong Xu: writing - reviewing and editing. Xiaoquan Wang: supervision, project administration, funding acquisition, conceptualization, investigation, methodology, validation, writing - reviewing and editing. Xiufan Liu: supervision, project administration, funding acquisition, conceptualization.

Conflict of interest

No potential conflict of interest was reported by the authors.

Acknowledgments

This work was supported by the National Key Research and Development Project of China: 2021YFD1800202; by the National Natural Science Foundation of China: 31772755, 32072892, 32072832; by the Earmarked Fund for China Agriculture Reasearch System: CARS-40 and by the Priorty Academic Program Development of Jiangsu Higher Education Institutions (PAPD).

Appendix A. Supplementary data

Supplementary data to this article can be found online at https://doi.org/10.1016/j.virs.2022.09.006.

References

Alexander, D.J., 2003. Report on avian influenza in the eastern hemisphere during 1997-2002. Avian Dis. 47, 792–797.
Arai, Y., Kawashita, N., Ibrahim, M.S., Elgendy, E.M., Daidoji, T., Ono, T., Takagi, T., Nakaya, T., Matsumoto, K., Watanabe, Y., 2019. PB2 mutations arising during H9N2 influenza evolution in the Middle East confer enhanced replication and growth in mammals. PLoS Pathog. 15, e1007919.
Bi, Y., Chen, Q., Wang, Q., Chen, J., Jin, T., Wong, G., Quan, C., Liu, J., Wu, J., Yin, R., Zhao, L., Li, M., Ding, Z., Zou, R., Xu, W., Li, H., Wang, H., Tian, K., Fu, G., Huang, Y., Shestopalov, A., Li, S., Xu, B., Yu, H., Luo, T., Lu, L., Xu, X., Luo, Y., Liu, Y., Shi, W., Liu, D., Gao, G.F., 2016. Genesis, evolution and prevalence of H5N6 avian influenza viruses in China. Cell Host Microbe 20, 810–821.
Bi, Y., Li, J., Li, S., Fu, G., Jin, T., Zhang, C., Yang, Y., Ma, Z., Tian, W., Li, J., Xiao, S., Li, L., Yin, R., Zhang, Y., Wang, L., Qin, Y., Yao, Z., Meng, F., Hu, D., Li, D., Wong, G., Liu, F., Lv, N., Wang, L., Fu, L., Yang, Y., Peng, Y., Ma, J., Sharshov, K., Shestopalov, A., Gulyaeva, M., Gao, G.F., Chen, J., Shi, Y., Liu, W.J., Chu, D., Huang, Y., Liu, Y., Liu, L., Liu, W., Chen, Q., Shi, W., 2020. Dominant subtype switch in avian influenza viruses during 2016-2019 in China. Nat. Commun. 11, 5909.
Bisset, A.T., Hoyne, G.F., 2020. Evolution and adaptation of the avian H7N9 virus into the human host. Microorganisms 8, 778.
Chen, H., Yuan, H., Gao, R., Zhang, J., Wang, D., Xiong, Y., Fan, G., Yang, F., Li, X., Zhou, J., Zou, S., Yang, L., Chen, T., Dong, L., Bo, H., Zhao, X., Zhang, Y., Lan, Y., Bai, T., Dong, J., Li, Q., Wang, S., Zhang, Y., Li, H., Gong, T., Shi, Y., Ni, X., Li, J., Zhou, J., Fan, J., Wu, J., Zhou, X., Hu, M., Wan, J., Yang, W., Li, D., Wu, G., Feng, Z., Gao, G.F., Wang, Y., Jin, Q., Liu, M., Shu, Y., 2014. Clinical and epidemiological characteristics of a fatal case of avian influenza A H10N8 virus infection: a descriptive study. Lancet 383, 714–721.
Chen, Y., Liang, W., Yang, S., Wu, N., Gao, H., Sheng, J., Yao, H., Wo, J., Fang, Q., Cui, D., Li, Y., Yao, X., Zhang, Y., Wu, H., Zheng, S., Diao, H., Xia, S., Zhang, Y., Chan, K.H., Tsoi, H.W., Teng, J.L., Song, W., Wang, P., Lau, S.Y., Zheng, M., Chan, J.F., To, K.K., Chen, H., Li, L., Yuen, K.Y., 2013. Human infections with the emerging avian influenza A H7N9 virus from wet market poultry: clinical analysis and characterisation of viral genome. Lancet 381, 1916–1925.
Ciminski, K., Chase, G.P., Beer, M., Schwemmle, M., 2021. Influenza A viruses: understanding human host determinants. Trends Mol. Med. 27, 104–112.
De Vries, R.P., Peng, W., Grant, O.C., Thompson, A.J., Zhu, X., Bouwman, K.M., De La Pena, A.T.T., Van Breemen, M.J., Ambepitiya Wickramasinghe, I.N., De Haan, C.A.M., Yu, W., Mcbride, R., Sanders, R.W., Woods, R.J., Verheije, M.H., Wilson, I.A., Paulson, J.C., 2017a. Three mutations switch H7N9 influenza to human-type receptor specificity. PLoS Pathog. 13, e1006390.
De Vries, R.P., Tzarum, N., Peng, W., Thompson, A.J., Ambepitiya Wickramasinghe, I.N., De La Pena, A.T.T., Van Breemen, M.J., Bouwman, K.M., Zhu, X., Mcbride, R., Yu, W., Sanders, R.W., Verheije, M.H., Wilson, I.A., Paulson, J.C., 2017b. A single mutation in Taiwanese H6N1 influenza hemagglutinin switches binding to human-type receptors. EMBO Mol. Med. 9, 1314–1325.
Ge, Y., Yao, Q., Chai, H., Hua, Y., Deng, G., Chen, H., 2018. A 627K variant in the PB2 protein of H9 subtype influenza virus in wild birds. Influenza Other Respir Viruses 12, 728–741.

Gu, J., Gu, M., Yan, Y., Liu, K., Wang, X., Xu, X., Liu, X., 2020. Detection of PB2 627K mutation in two highly pathogenic isolates of the H7N9 subtype Influenza a virus from chickens in Northern China. J. Infect. 81, 979–997.
Guan, Y., Shortridge, K.F., Krauss, S., Webster, R.G., 1999. Molecular characterization of H9N2 influenza viruses: were they the donors of the "internal" genes of H5N1 viruses in Hong Kong? Proc. Natl. Acad. Sci. U. S. A 96, 9363–9367.
Guo, J., Wang, Y., Zhao, C., Gao, X., Zhang, Y., Li, J., Wang, M., Zhang, H., Liu, W., Wang, C., Xia, Y., Xu, L., He, G., Shen, J., Sun, X., Wang, W., Han, X., Zhang, X., Hou, Z., Jin, X., Peng, N., Li, Y., Deng, G., Cui, P., Zhang, Q., Li, X., Chen, H., 2021. Molecular characterization, receptor binding property, and replication in chickens and mice of H9N2 avian influenza viruses isolated from chickens, peafowls, and wild birds in eastern China. Emerg. Microb. Infect. 10, 2098–2112.
Hao, X., Hu, J., Wang, X., Gu, M., Wang, J., Liu, D., Gao, Z., Chen, Y., Gao, R., Li, X., Hu, Z., Hu, S., Liu, X., Peng, D., Jiao, X., Liu, X., 2019. The PB2 and M genes are critical for the superiority of genotype S H9N2 virus to genotype H in optimizing viral fitness of H5Nx and H7N9 avian influenza viruses in mice. Transbound Emerg Dis 67, 758–768.
Hatta, M., Gao, P., Halfmann, P., Kawaoka, Y., 2001. Molecular basis for high virulence of Hong Kong H5N1 influenza A viruses. Science 293, 1840–1842.
Hayden, F.G., Cote, K., Douglas, R.G., 1980. Plaque inhibition assay for drug susceptibility testing of influenza viruses. Antimicrob. Agents Chemother. 17, 865–870.
Hoa, L.N.M., Tuan, N.A., My, P.H., Huong, T.T.K., Chi, N.T.Y., Hau Thu, T.T., Carrique-Mas, J., Duong, M.T., Tho, N.D., Hoang, N.D., Thanh, T.L., Diep, N.T., Duong, N.V., Toan, T.K., Tung, T.S., Mai, L.Q., Iqbal, M., Wertheim, H., Van Doorn, H.R., Bryant, J.E., The Vizions, C., 2017. Assessing evidence for avian-to-human transmission of influenza A/H9N2 virus in rural farming communities in northern Vietnam. J. Gen. Virol. 98, 2011–2016.
Hoffmann, E., Neumann, G., Kawaoka, Y., Hobom, G., Webster, R.G., 2000. A DNA transfection system for generation of influenza A virus from eight plasmids. Proc. Natl. Acad. Sci. U. S. A. 97, 6108–6113.
Hoffmann, E., Stech, J., Guan, Y., Webster, R., Perez, D., 2001. Universal primer set for the full-length amplification of all influenza A viruses. Arch. Virol. 146, 2275–2289.
Homme, P.J., Easterday, B.C., 1970. Avian influenza virus infections. I. Characteristics of influenza A-Turkey-Wisconsin-1966 virus. Avian Dis. 14, 66–74.
Khan, S.U., Anderson, B.D., Heil, G.L., Liang, S., Gray, G.C., 2015. A systematic review and meta-analysis of the seroprevalence of influenza A(H9N2) infection among humans. J. Infect. Dis. 212, 562–569.
Klumpp, K., Ruigrok, R.W., Baudin, F., 1997. Roles of the influenza virus polymerase and nucleoprotein in forming a functional RNP structure. EMBO J. 16, 1248–1257.
Kong, H., Ma, S., Wang, J., Gu, C., Wang, Z., Shi, J., Deng, G., Guan, Y., Chen, H., 2019. Identification of key amino acids in the PB2 and M1 proteins of H7N9 influenza virus that affect its transmission in Guinea pigs. J. Virol. 94, e01180–19.
Kong, X., Guan, L., Shi, J., Kong, H., Zhang, Y., Zeng, X., Tian, G., Liu, L., Li, C., Kawaoka, Y., Deng, G., Chen, H., 2021. A single-amino-acid mutation at position 225 in hemagglutinin attenuates H5N6 influenza virus in mice. Emerg. Microb. Infect. 10, 2052–2061.
Li, Q., Wang, X., Gu, M., Zhu, J., Hao, X., Gao, Z., Sun, Z., Hu, J., Hu, S., Wang, X., 2014a. Novel H5 clade 2.3.4.6 viruses with both α-2,3 and α-2,6 receptor binding properties may pose a pandemic threat. Vet. Res. 45, 1–6.
Li, Q., Wang, X., Zhong, L., Wang, X., Sun, Z., Gao, Z., Cui, Z., Zhu, J., Gu, M., Liu, X., Liu, X., 2014b. Adaptation of a natural reassortant H5N2 avian influenza virus in mice. Vet. Microbiol. 172, 568–574.
Li, X., Shi, J., Guo, J., Deng, G., Zhang, Q., Wang, J., He, X., Wang, K., Chen, J., Li, Y., Fan, J., Kong, H., Gu, C., Guan, Y., Suzuki, Y., Kawaoka, Y., Liu, L., Jiang, Y., Tian, G., Li, Y., Bu, Z., Chen, H., 2014c. Genetics, receptor binding property, and transmissibility in mammals of naturally isolated H9N2 Avian Influenza viruses. PLoS Pathog. 10, e1004508.
Liang, L., Jiang, L., Li, J., Zhao, Q., Wang, J., He, X., Huang, S., Wang, Q., Zhao, Y., Wang, G., Sun, N., Deng, G., Shi, J., Tian, G., Zeng, X., Jiang, Y., Liu, L., Liu, J., Chen, P., Bu, Z., Kawaoka, Y., Chen, H., Li, C., 2019. Low polymerase activity attributed to PA drives the acquisition of the PB2 E627K mutation of H7N9 avian influenza virus in mammals. mBio 10, e01162–19.
Linster, M., Van Boheemen, S., De Graaf, M., Schrauwen, E.J.A., Lexmond, P., Manz, B., Bestebroer, T.M., Baumann, J., Van Riel, D., Rimmelzwaan, G.F., Osterhaus, A., Matrosovich, M., Fouchier, R.A.M., Herfst, S., 2014. Identification, characterization, and natural selection of mutations driving airborne transmission of A/H5N1 virus. Cell 157, 329–339.
Liu, K., Ding, P., Pei, Y., Gao, R., Han, W., Zheng, H., Ji, Z., Cai, M., Gu, J., Li, X., Gu, M., Hu, J., Liu, X., Hu, S., Zhang, P., Wang, X., Wang, X., Liu, X., 2022. Emergence of a novel reassortant avian influenza virus (H10N3) in Eastern China with high pathogenicity and respiratory droplet transmissibility to mammals. Sci. China Life Sci. 65, 1024–1035.
Liu, K., Wang, X., Jiang, D., Xu, N., Gao, R., Han, W., Gu, M., Hu, J., Liu, X., Hu, S., Liu, X., 2021. Pathogenicity and transmissibility of an H9N2 avian influenza virus that naturally harbors the mammalian-adaptive molecular factors in the hemagglutinin and PB2 proteins. J. Infect. 82, e22–e23.
Liu, X., Yang, C., Sun, X., Lin, X., Zhao, L., Chen, H., Jin, M., 2019. Evidence for a novel mechanism of influenza A virus host adaptation modulated by PB2-627. FEBS J. 286, 3389–3400.
Liu, Y., Li, S., Sun, H., Pan, L., Cui, X., Zhu, X., Feng, Y., Li, M., Yu, Y., Wu, M., Lin, J., Xu, F., Yuan, S., Huang, S., Sun, H., Liao, M., 2020. Variation and molecular basis for enhancement of receptor binding of H9N2 avian influenza viruses in China isolates. Front. Microbiol. 11, 602124.
Long, J.S., Mistry, B., Haslam, S.M., Barclay, W.S., 2019. Host and viral determinants of influenza A virus species specificity. Nat. Rev. Microbiol. 17, 67–81.
Ma, S., Zhang, B., Shi, J., Yin, X., Wang, G., Cui, P., Liu, L., Deng, G., Jiang, Y., Li, C., Chen, H., 2020. Amino acid mutations A286V and T437M in the nucleoprotein attenuate H7N9 viruses in mice. J. Virol. 94, e01530–19.
Mair, C.M., Ludwig, K., Herrmann, A., Sieben, C., 2014. Receptor binding and pH stability — how influenza A virus hemagglutinin affects host-specific virus infection. Biochim. Biophys. Acta Biomembr. 1838, 1153–1168.
Matrosovich, M., Tuzikov, A., Bovin, N., Gambaryan, A., Klimov, A., Castrucci, M.R., Donatelli, I., Kawaoka, Y., 2000. Early alterations of the receptor-binding properties of H1, H2, and H3 avian influenza virus hemagglutinins after their introduction into mammals. J. Virol. 74, 8502–8512.
Mok, C.K., Lee, H.H., Lestra, M., Nicholls, J.M., Chan, M.C., Sia, S.F., Zhu, H., Poon, L.L., Guan, Y., Peiris, J.S., 2014. Amino acid substitutions in polymerase basic protein 2 gene contribute to the pathogenicity of the novel A/H7N9 influenza virus in mammalian hosts. J. Virol. 88, 3568–3576.
Neumann, G., Kawaoka, Y., 2006. Host range restriction and pathogenicity in the context of influenza pandemic. Emerg. Infect. Dis. 12, 881–886.
Ning, Z.Y., Luo, M.Y., Qi, W.B., Yu, B., Jiao, P.R., Liao, M., 2009. Detection of expression of influenza virus receptors in tissues of BALB/c mice by histochemistry. Vet. Res. Commun. 33, 895–903.
Peacock, T.H.P., James, J., Sealy, J.E., Iqbal, M., 2019. A global perspective on H9N2 avian influenza virus. Viruses 11, 620.
Peacock, T.P., Sealy, J.E., Harvey, W.T., Benton, D.J., Reeve, R., Iqbal, M., 2020. Genetic determinants of receptor-binding preference and zoonotic potential of H9N2 avian influenza viruses. J. Virol. 95, e01651–20.
Peiris, M., Yuen, K.Y., Leung, C.W., Chan, K.H., Ip, P.L.S., Lai, R.W.M., Orr, W.K., Shortridge, K.F., 1999. Human infection with influenza H9N2. Lancet 354, 916–917.
Pu, J., Wang, S., Yin, Y., Zhang, G., Carter, R.A., Wang, J., Xu, G., Sun, H., Wang, M., Wen, C., Wei, Y., Wang, D., Zhu, B., Lemmon, G., Jiao, Y., Duan, S., Wang, Q., Du, Q., Sun, M., Bao, J., Sun, Y., Zhao, J., Zhang, H., Wu, G., Liu, J., Webster, R.G., 2015. Evolution of the H9N2 influenza genotype that facilitated the genesis of the novel H7N9 virus. Proc. Natl. Acad. Sci. U. S. A. 112, 548–553.
Reed, L.J., Muench, H., 1938. A simple method of estimating fifty per cent endpoints. Am. J. Epidemiol. 27, 493–497.
Shen, Y.Y., Ke, C.W., Li, Q., Yuan, R.Y., Xiang, D., Jia, W.X., Yu, Y.D., Liu, L., Huang, C., Qi, W.B., Sikkema, R., Wu, J., Koopmans, M., Liao, M., 2016. Novel reassortant avian influenza A(H5N6) viruses in humans, guangdong, China, 2015. Emerg. Infect. Dis. 22, 1507–1509.
Shi, J., Deng, G., Kong, H., Gu, C., Ma, S., Yin, X., Zeng, X., Cui, P., Chen, Y., Yang, H., Wan, X., Wang, X., Liu, L., Chen, P., Jiang, Y., Liu, J., Guan, Y., Suzuki, Y., Li, M., Qu, Z., Guan, L., Zang, J., Gu, W., Han, S., Song, Y., Hu, Y., Wang, Z., Gu, L., Yang, W., Liang, L., Bao, H., Tian, G., Li, Y., Qiao, C., Jiang, L., Li, C., Bu, Z., Chen, H., 2017. H7N9 virulent mutants detected in chickens in China pose an increased threat to humans. Cell Res. 27, 1409–1421.
Shi, Y., Wu, Y., Zhang, W., Qi, J., Gao, G.F., 2014. Enabling the 'host jump': structural determinants of receptor-binding specificity in influenza A viruses. Nat. Rev. Microbiol. 12, 822–831.
Shinya, K., Ebina, M., Yamada, S., Ono, M., Kasai, N., Kawaoka, Y., 2006. Influenza virus receptors in the human airway. Nature 440, 435–436.
Song, H., Qi, J., Xiao, H., Bi, Y., Zhang, W., Xu, Y., Wang, F., Shi, Y., Gao, G.F., 2017. Avian-to-Human receptor-binding adaptation by influenza A virus hemagglutinin H4. Cell Rep. 20, 1201–1214.
Song, W., Wang, P., Mok, B.W., Lau, S.Y., Huang, X., Wu, W.L., Zheng, M., Wen, X., Yang, S., Chen, Y., Li, L., Yuen, K.Y., Chen, H., 2014. The K526R substitution in viral protein PB2 enhances the effects of E627K on influenza virus replication. Nat. Commun. 5, 5509.
Stevens, J., Blixt, O., Tumpey, T.M., Taubenberger, J.K., Paulson, J.C., Wilson, I.A., 2006. Structure and receptor specificity of the hemagglutinin from an H5N1 influenza virus. Science 312, 404–410.
Sun, X., Belser, J.A., Maines, T.R., 2020. Adaptation of H9N2 influenza viruses to mammalian hosts: a review of molecular markers. Viruses 12, 541.
Taubenberger, J.K., Kash, J.C., 2010. Influenza virus evolution, host adaptation, and pandemic formation. Cell Host Microbe 7, 440–451.
Teng, Q., Xu, D., Shen, W., Liu, Q., Rong, G., Li, X., Yan, L., Yang, J., Chen, H., Yu, H., Ma, W., Li, Z., 2016. A single mutation at position 190 in hemagglutinin enhances binding affinity for human type sialic acid receptor and replication of H9N2 avian influenza virus in mice. J. Virol. 90, 9806–9825.
Thompson, A.J., Paulson, J.C., 2021. Adaptation of influenza viruses to human airway receptors. J. Biol. Chem. 296, 100017.
Van Hoeven, N., Pappas, C., Belser, J.A., Maines, T.R., Zeng, H., Garcia-Sastre, A., Sasisekharan, R., Katz, J.M., Tumpey, T.M., 2009. Human HA and polymerase subunit PB2 proteins confer transmission of an avian influenza virus through the air. Proc. Natl. Acad. Sci. U. S. A. 106, 3366–3371.
Walther, T., Karamanska, R., Chan, R.W., Chan, M.C., Jia, N., Air, G., Hopton, C., Wong, M.P., Dell, A., Malik Peiris, J.S., Haslam, S.M., Nicholls, J.M., 2013. Glycomic analysis of human respiratory tract tissues and correlation with influenza virus infection. PLoS Pathog. 9, e1003223.
Watanabe, T., Zhong, G., Russell, C.A., Nakajima, N., Hatta, M., Hanson, A., Mcbride, R., Burke, D.F., Takahashi, K., Fukuyama, S., Tomita, Y., Maher, E.A., Watanabe, S., Imai, M., Neumann, G., Hasegawa, H., Paulson, J.C., Smith, D.J., Kawaoka, Y., 2014. Circulating avian influenza viruses closely related to the 1918 virus have pandemic potential. Cell Host Microbe 15, 692–705.
WHO. Avian Influenza Weekly Update 2022. https://www.who.int/westernpacific/emergencies/surveillance/avian-influenza. (Accessed 26 July 2022).
Zhang, Q., Shi, J., Deng, G., Guo, J., Zeng, X., He, X., Kong, H., Gu, C., Li, X., Liu, J., Wang, G., Chen, Y., Liu, L., Liang, L., Li, Y., Fan, J., Wang, J., Li, W., Guan, L., Li, Q., Yang, H., Chen, P., Jiang, L., Guan, Y., Xin, X., Jiang, Y., Tian, G., Wang, X., Qiao, C., Li, C., Bu, Z., Chen, H., 2013. H7N9 influenza viruses are transmissible in ferrets by respiratory droplet. Science 341, 410.